Nanotechnology

Direct observation of tunnelled intergrowth in SnO_2/Ga_2O_3 Complex Nanowires

To cite this article before publication: Oliver M Rigby *et al* 2018 *Nanotechnology* in press https://doi.org/10.1088/1361-6528/aaefc4

IOP Publishing Nanotechnology
Nanotechnol. **XX** (XXXX) XXXXXX https://doi.org/XXXX/XXXX

Direct Observation of Tunnelled Intergrowth in SnO_2/Ga_2O_3 Complex Nanowires

Oliver M. Rigby[1], Alice V. Stamp[1], Steve A. Hindmarsh[1], Manuel Alonso-Orts[2], Emilio Nogales[2], Bianchi Méndez[2] and Ana M. Sanchez[†1]

[1] Department of Physics, University of Warwick, Coventry, CV4 7AL, United Kingdom
[2] Departamento Fisica de Materiales, Facultad de CC Fisicas, Universidad Complutense de Madrid, 28040 Madrid, Spain

[†]E-mail: a.m.sanchez@warwick.ac.uk

Received xxxxxx
Accepted for publication xxxxxx
Published xxxxxx

Abstract

β- Ga_2O_3 intergrowths have been revealed in the SnO_2 rutile structure when SnO_2/Ga_2O_3 complex nanostructures are grown by thermal evaporation with a catalyst-free basis method. The structure is formed by a Ga_2O_3 nanowire trunk, around which a rutile SnO_2 particle is formed with [001] aligned to the [010] Ga_2O_3 trunk axis. Inside the SnO_2 particle, β- Ga_2O_3 units occur separated periodically by hexagonal tunnels in the (210) rutile plane. Orange (620 nm) optical emission from tin oxide, with a narrow linewidth indicating localized electronic states, may be associated with this β-Ga_2O_3 intergrowth.

Keywords: wide band gap oxides, transmission electron microscopy, tunnelled intergrowth

1. Introduction

Significant advances in semiconducting metal oxides for optoelectronic applications have been recently reported[1]. The wide band gap of the monoclinic β-Ga_2O_3 (4.9 eV) and rutile SnO_2 (3.7 eV), make these metal oxides suitable for applications in the ultraviolet range. These thermodynamically stable phases are easy to produce and chemically stable. Additionally, Ga and Sn are more abundant than e.g. indium in the Earth's upper continental crust[2, 3] providing a potential alternative to rare-metal free transistors[3]. These oxides offer a wide range of optoelectronic applications including photodetectors[4], solar cells[5], photocatalysis[6] and biomedical usages[7, 8].

Currently, nanoscale structures are at the forefront of research. New architectures of mixed dimensionality and materials combination open up new and versatile applications. Our previous work has clearly demonstrated the growth of complex oxide structures, based on Ga_2O_3 and SnO_2 using thermal evaporation and careful choice of growth parameters (gas flow, temperature and Cr doping)[9-11]. Different architectures have been reported involving these two metal oxides, which constitute the first steps in the design of novel hierarchical oxide nanostructures with wide band gap and tailored functionalities.

Previous work showed that β-Ga_2O_3 reacts with oxides possessing the rutile structure to form coherent intergrowths[12-15]. These structures can be described as sheets of β-Ga_2O_3 between slabs of rutile (SnO_2, GeO_2, or TiO_2)[16]. Here, we report the observation of similar tunnelled intergrowth structures in a SnO_2/Ga_2O_3 nanostructure. In our case, the intergrowth of Ga_2O_3 sheets in SnO_2 produces 1-D hexagonal tunnels lying parallel to the *b*-axis of the intergrowth. These tunnels may be suitable hosts for small-to-medium cations[17], with potential application as battery electrodes, or strongly anisotropic ionic conductors. In addition to studying the intergrowth structure, we also use cathodoluminescence (CL) to shed some light on previously unreported luminescence bands of tin oxide.

2. Materials and Methods

Ga_2O_3/SnO_2 nanostructures were synthesized via catalyst-free thermal evaporation. The precursor material was a mixture of 90 wt.% Ga_2O_3 and 10 wt.% SnO_2 powders compacted into a disk of 5 mm diameter. Some pure metallic Ga was placed on the upper surface of the pellet to enhance the growth of Ga_2O_3 nanowires. The pellet was introduced into a furnace and heated under flowing argon for 8 hours at 1100 ^oC. The formation mechanism is a vapor-solid process, which produces many nanostructures on the pellet surface. Most structures have a characteristic morphology of a Ga_2O_3 nanowire, or trunk, decorated with small SnO_2 particles around, in a skewer-like (SK) arrangement. In previous work we studied SK structures formed by adding tin oxide powders on a pure gallium oxide pellet[10] instead of incorporating them into the substrate. We show here that such slight changes in the sample preparation procedure can alter the microstructure of the final product.

The SK nanostructures were transferred into a TEM copper grid with a lacy carbon support for scanning electron microscopy (SEM) characterization and cathodoluminescence (CL) spectroscopy, using a Gatan MonoCL4 spectrometer attached to a Zeiss Supra 55VP SEM operating at 10 kV (using a spectral resolution of 5nm). Focused ion beam (FIB) sections of selected SK nanostructures were fabricated in a JEOL 4500 FIB-SEM and characterized by scanning transmission electron microscopy (STEM) in a doubly-corrected JEOL ARM200F working at 200 kV. Energy dispersive X-ray spectroscopy (EDX) analyses in STEM mode were performed with probe currents of approximately 200 pA and a windowless Oxford Instruments X-Max Silicon Drift Detector with an area of 100 mm^2.

3. Results and discussion

Fig. 1 (a) shows a secondary electron image of a typical SK structure. An elemental EDX map (Sn orange, Ga yellow) confirms that the thin Ga_2O_3 nanowires (<100nm diameter) thread through the larger SnO_2 particles. As we demonstrate below (Fig. 3b) the Ga_2O_3 NW axis is [010], parallel to the [001] direction of the SnO_2 particles. The SnO_2 particles have well-defined facets, with characteristic (100) and (101) planes. This does not fully agree with the theoretical calculations for SnO_2 surface energies[18, 19] that predict that the (110) rutile surface has the lowest energy, and is therefore the most stable thermodynamically. The calculated sequence for the surface stability in the SnO_2 rutile is (110)<(010)<(101)<(001). Nevertheless, the formation of SnO_2 crystals with (101) facet planes has been previously reported[20]. Using vapor-solid growth and different temperatures, Zhou et al[20] were able to tune the {**101**} facet ratios of SnO_2 polyhedra, demonstrating similar structures to the SnO_2 particles grown on the Ga_2O_3 nanowires reported in this article.

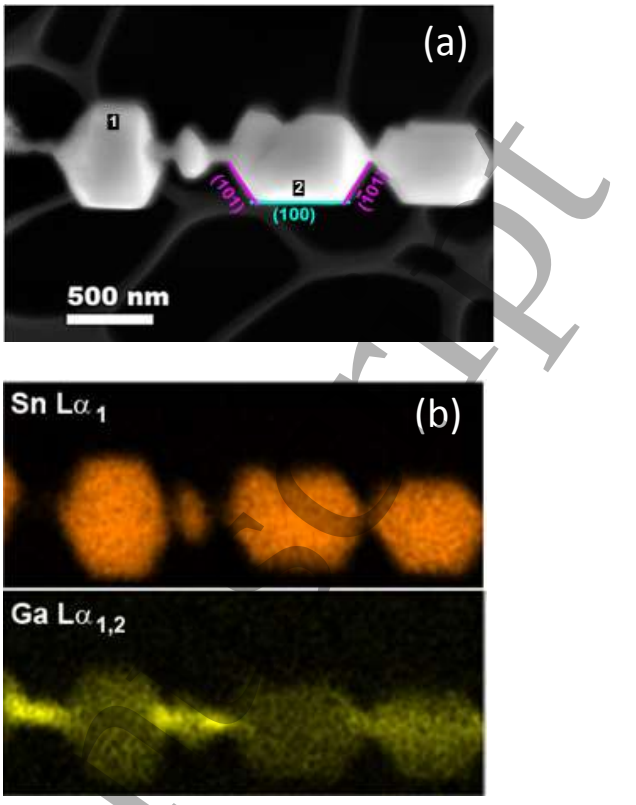

Fig. 1 (a) Secondary electron SEM image of the SnO_2/Ga_2O_3 structure. *1* and *2* indicate the points where the cathodoluminescence spectra were taken. SnO_2 polyhedron facets are also indicated. (b) and (c) EDS mapping for the Sn and Ga respectively.

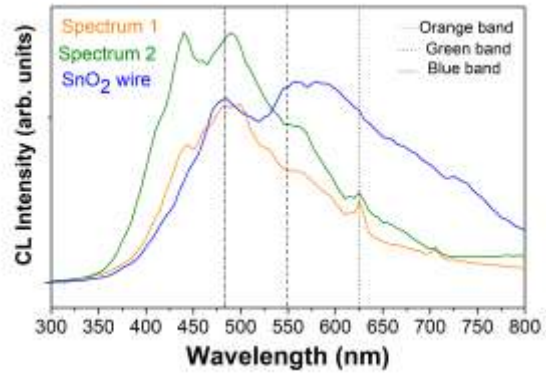

Fig. 2 Comparative room temperature CL spectra of the SnO_2 particles recorded at points *1* and *2* marked in Fig. 1a. CL spectrum from SnO_2 wire is also shown.

Fig. 2 shows room temperature CL spectra recorded from the SnO_2 particles at points *1* and *2* in Fig. 1a and compared with the spectrum recorded from a SnO_2 wire taken as a reference. SnO_2 usually contains a high number of oxygen vacancies that are responsible for its complex luminescence features. Furthermore, in the case of small particles the large surface/volume ratio may affect luminescence properties.

Here, we observe that the isolated SnO_2 wire displays luminescence involving broad green-blue (~480 nm) and orange (580-620 nm) emission bands (blue line in Fig. 2). These components have been reported in SnO_2 nanowires and in sintered SnO_2. The orange emission is usually attributed to oxygen vacancies and/or related states, while coupling of surface states with oxygen vacancies have been proposed for the green-blue emission[21,22]. In the case of SnO_2 particles, we find that the CL spectra (red and green lines) from points *1* and *2* in Fig.1. show two distinct features in comparison with the isolated SnO_2 wire. First, the dominant luminescence is the blue-green band, which is consistent with the role that surface states play in this emission. And, on the other hand, the broad orange band is replaced by a narrow emission line at 620 nm. Previous photoluminescence (PL) studies in SnO_2 nanoribbons obtained by laser ablation reporteda strong broad luminescence peak around 620 nm[23-25] associated with oxygen vacancy – tin interstitials leading to formation of trapped states in the bandgap[25]. Here, we observe that orange emission narrows, what suggests local changes in the electronic levels probably as a consequence of changes of the local crystal microstructure of the SnO_2 particles attached to the Ga_2O_3 nanowire. In order to elucidate this point, we have carried out high-resolution transmission electron microscopy in a cross-section of the SK SnO_2/Ga_2O_3 nanostructures.

A focused ion beam (FIB) section perpendicular to the axis of the Ga_2O_3 nanowire and containing one of the SnO2 particles was fabricated. A low magnification annular dark field (ADF) image of this section is shown in Fig. 3a, showing the Ga_2O_3 nanowire centered in the SnO_2 particle. To determine the crystallographic relationship of the Ga_2O_3/SnO_2 heterojunction, high magnification ADF images were recorded such as the one shown in Fig. 3b. Here, the projection indicates that the [010] Ga_2O_3 axis is parallel to [001] SnO_2. This orientation relationship is slightly different to previous investigations of similar growths, in which Ga_2O_3 nanowires had a [$\bar{1}$**10**] axis[10,11]. Both orientations are quite common in Ga_2O_3 due to the anisotropy of the lattice in the *b* direction. In the current case the Ga_2O_3 nanowires with a [010] axis act as a lattice-matched substrate for the SnO_2[10].

Dark lines, marking boundaries along {**210**} planes[12] of the SnO_2 (e.g. marked by a green square in Fig. 3b) were observed. Antiphase[26] and twin[27] boundaries in SnO_2 have been reported previously. Nevertheless, the atomic structure of the dark lines does not correspond with either of these defects, since it cannot be described as a simple displacement of the SnO_2 crystal lattice. Hexagonal tunnels, with a diameter < 3 Å and period of approx. 1 nm, can be seen in the boundaries. To get a better understanding of these boundaries, EDX elemental mapping was recorded as shown in Fig. 4a. Here, two dark boundaries are separated by six unit cells of SnO_2.

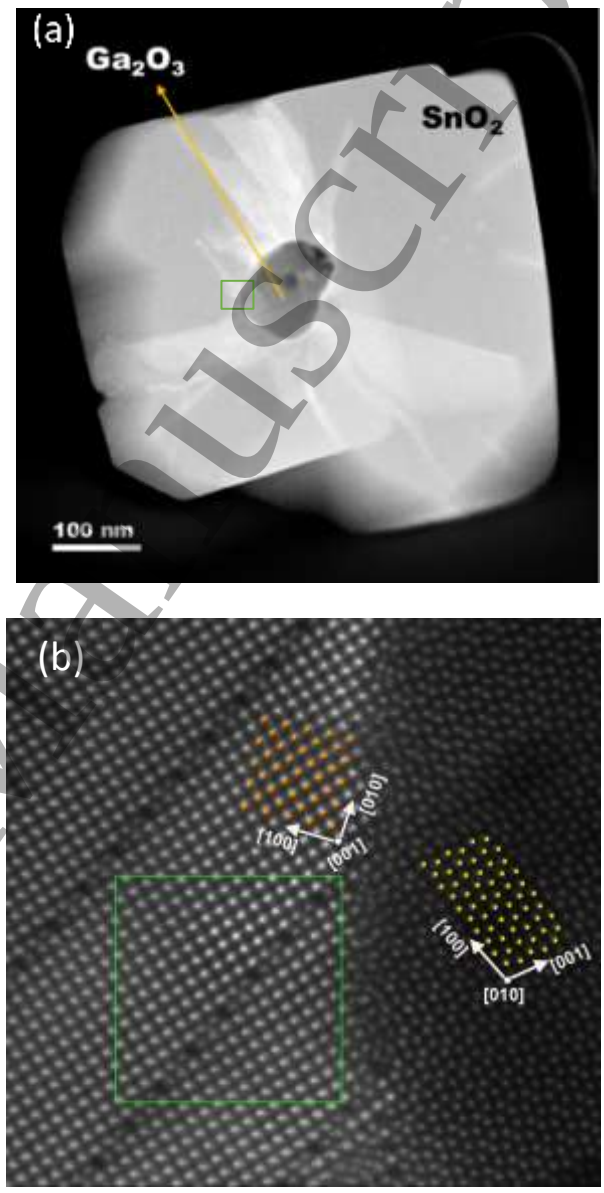

Fig. 3. (a) Low magnification ADF-STEM cross-section image of the area of the SK structure prepared by FIB. (b) Atomic resolution ADF image of the heterojunction between the Ga_2O_3 nanowire and the SnO_2 particle, overlapped with the cation balls model for Ga_2O_3 (yellow) and SnO_2 (orange).

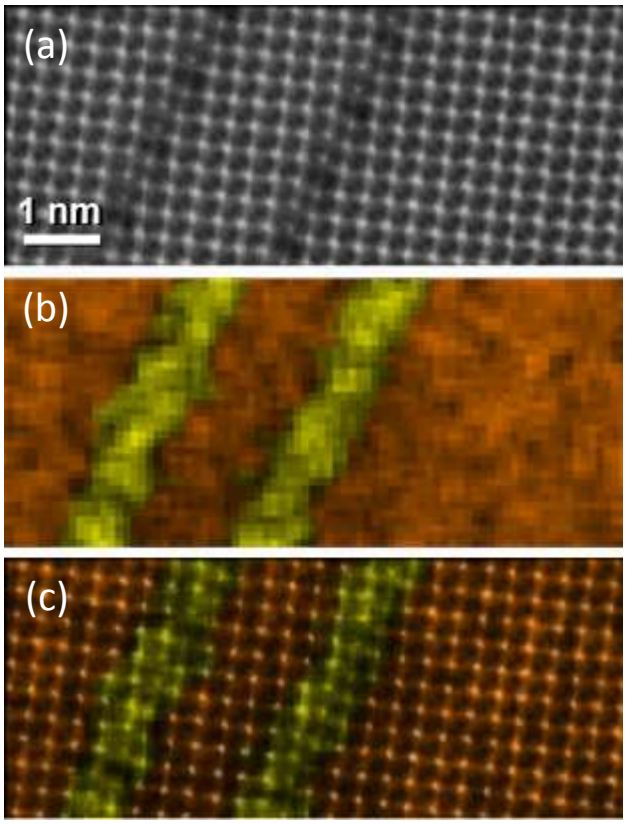

Fig. 4. (a) ADF image of an area of the SnO_2 particle containing Gallium intergrowth (b) Ga (yellow) and Sn (orange) overlaid EDS map of the same area. (c) superimposed ADF and EDS maps

This type of intergrowth was not observed in previous structures grown under similar conditions[9-11]. On the other hand, this tunnelled intergrowth of Ga_2O_3 into the SnO_2 could explain the luminescence features observed in Fig.2. It is known that deep centers associated with native defects, such as vacancies, have localized wave functions induced by the broken bonds and strain associated with the displacement of atoms. Here, the tunnelled intergrowth may modify the electronic states structure and promote the narrowing of the orange emission at 620 nm, which was not observed in single SnO_2 wires or in previous SnO_2 particles on Ga_2O_3 trunks. This may have been because the particular orientation relationship between the Ga_2O_3 trunk and SnO_2 particle was different. Single Ga_2O_3 nanowires can present several wire axis orientations, such as [010], [001], [110] or [40-1], usually depending on the synthesis route.[29,30] In our previous works, either [001] Ga_2O_3/[10-1] SnO_2 or [1-10] Ga_2O_3/[010] SnO_2 relationships were found, whereas in the current case the β-Ga_2O_3 [010] nanowire axis is aligned with SnO_2 [001] as demonstrated in Fig. 3b. The distribution of hexagonal tunnels in these structures make them good candidates to host ions and could serve as one-dimensional conduction pathways.[17]

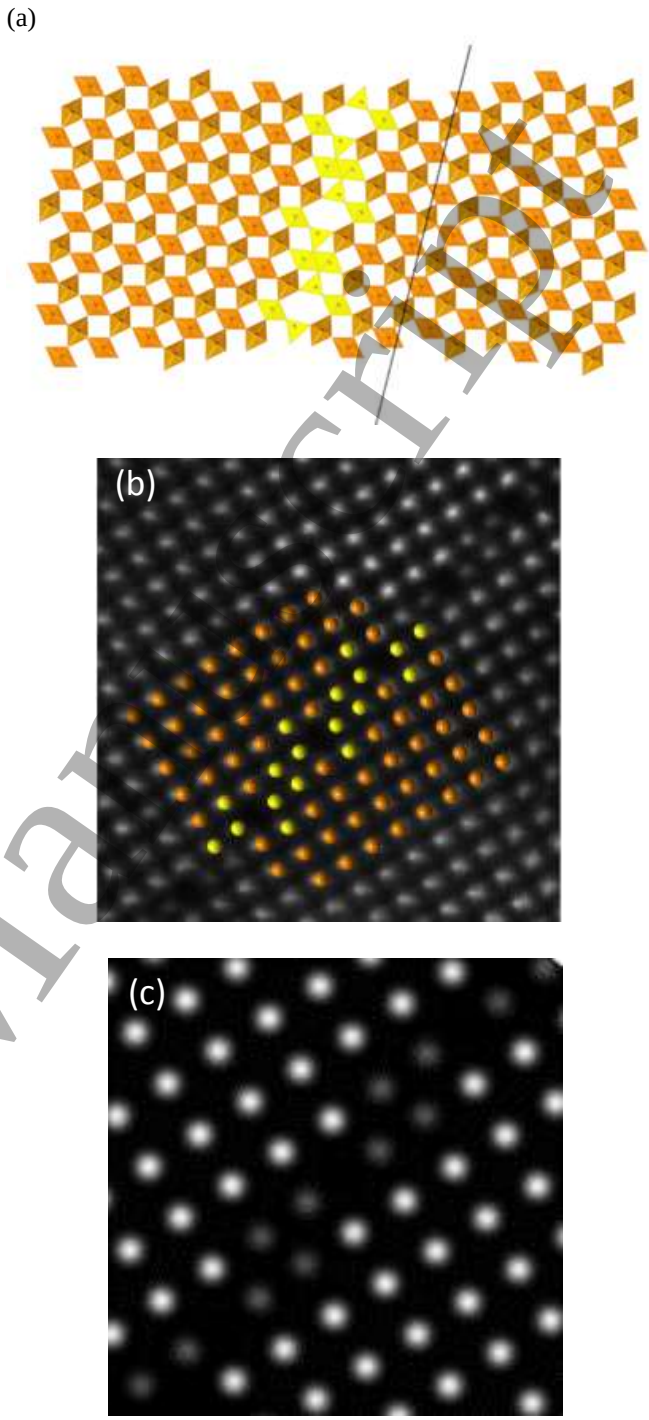

Fig. 5. (a) Structure of β-Ga_2O_3 columns (yellow) coherently incorporated in the rutile SnO_2 (orange). (b) Atomic resolution ADF images overlapped with ball model crystal intergrowth structure. Oxygen atoms are not shown in (b). (c)Multislice ADF simulation of the structure described in (a).

4. Conclusions

In summary, Ga_2O_3/SnO_2 material systems grown by thermal evaporation using a catalysis-free method showed β-Ga_2O_3 intergrowths in the SnO_2 rutile nanostructure formed around Ga_2O_3 nanowires. Electron microscopy shows planar β-Ga_2O_3 units separated by hexagonal tunnels with a diameter < 3 Å and period of approximately 1 nm in the (210) rutile plane. Room temperature cathodoluminescence emission was obtained in the SnO_2 particles. Blue and green luminescence dominates the spectrum because of the surface to volume ratio. In addition, the CL spectrum at selected points in the SnO_2 particles reveals a narrower orange band emission than previously observed in bulk-like material. The presence of gallium oxide mono-layers inside the tin oxide lattice could modify the electronic states and therefore the luminescence features.

Acknowledgements

We thank J.J.P.Peters for his input on the multislice ADF simulation. This work has been supported by MINECO projects MAT-2015-65274-R/FEDER and M-ERA.NET PCIN-2017-106. M. A- O acknowledges financial support from MECD (FPU contract).

References

[1] Yu X G, Marks T J and Facchetti A 2016 *Nat. Mater.* **15** 383
[2] Haxel G B, Hedrick J B, Orris G J, Stauffer P H and Hendley Ii J W 2002 *Rare earth elements: critical resources for high technology* 087-02
[3] Matsuda T, Umeda K, Kato Y, Nishimoto D, Furuta M and Kimura M 2017 *Scientific Reports* **7** 44326
[4] Lopez I, Castaldini A, Cavallini A, Nogales E, Mendez B and Piqueras J. 2014 *J. Phys. D-Appl. Phys.* **47** 6
[5] Abd-Ellah M, Bazargan S, Thomas J P, Rahman M A, Srivastava S, Wang X Y, Heinig N F and Leung K T 2015 *Adv. Electron. Mater.* **1** 6
[6] Jin S Q, Wang X, Wang X L, Ju M G, Shen S, Liang W Z, Zhao Y, Feng Z C, Playford H Y, Walton R I and Li C 2015 *J. Phys, Chem. C* **119** 18221
[7] Patolsky F, Zheng G, Hayden O, Lakadamyali M, Zhuang X and Lieber C M 2004 *Proc Natl Acad Sci U S A* **101** 14017
[8] Lieber C M and Wang Z L 2007 *MRS Bull.* **32** 99
[9] Mendez B, Lopez I, Alonso-Orts M, Sanz A, Nogales E, Hidalgo P and Piqueras J 2018 *Proc. of SPIE Nanotechnology Viii, Tiginyanu, I. M., Ed*. **10248** 1104805
[10] Alonso-Orts M, Sanchez A M, Hindmarsh S A, Lopez I, Nogales E, Piqueras J and Mendez B 2017 *Nano Lett.* **17** 515
[11] Alonso-Orts M, Sanchez A M, Lopez I, Nogales E, Piqueras J and Mendez B 2017 *CrystEngComm* **19** 6127
[12] Bursill L A and Stone G G 1981 *J. Solid State Chem.* **38** 149
[13] Edwards D D, Mason T O, Sinkler W, Marks L D, Poeppelmeier K R, Hu Z and Jorgensen J D 2000 *J. Solid State Chem* **150** 294
[14] Hervieu M, Desgardin G and Raveau B 1979 *J. Solid State Chem* **30** 375
[15] Turner, S.; Buseck, P. R. Science 1979, 203, (4379), 456-458.
[16] Lloyd D J, Grey I E and Bursill L A 1976 *Acta Crystallogr. Sect. B-Struct. Commun*. **32** 1756
[17] Empie N and Edwards D 2006 *Solid State Ion.* **177** 77
[18] Oviedo J and Gillan M J 2000 *Surf. Sci.* **463** 93
[19] Beltran A, Andres J, Longo E and Leite E R 2003 *Appl. Phys. Lett.* **83** 635
[20] Zhou G X, Wu X L, Liu L Z, Zhu X B, Zhu X S, Hao Y L and Chu P K 2015 *Appl. Surf. Sci.* **349** 798
[21] Luo S, Chu P K, Liu W, Zhang M and Lin C 2006 *Appl. Phys. Lett.* **88** 183112.
[22] Maestre D, Cremades A and Piqueras J 2005 *J. Appl. Phys.* **97** 044316
[23] Hadia N M A, Ryabtsev S V, Domashevskaya E P and Seredin P V 2009 *Eur. Phys. J. Appl. Phys.* **48** 1063
[24] Bonu V, Das A, Sardar M, Dhara S and Tyagi A K 2015 *J. Mat. Chem. C* **3** 1261
[25] Hu J Q, Bando Y, Liu Q L and Golberg D *Adv. Funct. Mat.* **13** 493
[26] Dominguez J E, Fu L and Pan X Q 2002 *Appl.Phys. Lett*. **81** 5168
[27] Zheng J G, Pan X Q, Schweizer M, Zhou F, Weimer U, Gopel W and Ruhle M 1996 *J. Appl. Phys.* **79** 7688
[28] Kahn A, Agafonov V, Michel D and Jorba M P Y 1986 *J. Solid State Chem* **65** 377
[29] Chun, H. J.; Choi, Y. S.; Bae, S. Y.; Seo, H. W.; Hong, S. J.; Park, J.; Yang, H. *J. Phys. Chem. B* **2003,** 107, 9042–9046.
[30] Hosein, I. D.; Hegde, M.; Jones, P. D.; Chirmanov, V.; Radovanovic, P. V. *J. Cryst. Growth* **2014,** 396, 24–32.